Garcia, R., Hajirasouliha, I., & Pilakoutas, K. (2010) "Seismic behaviour of deficient RC frames strengthened with CFRP composites", *Engineering Structures*, 32(10), 3075-3085. DOI: 10.1016/j.engstruct.2010.05.026

SEISMIC BEHAVIOUR OF DEFICIENT RC FRAMES STRENGTHENED WITH CFRP COMPOSITES

Reyes Garcia [*a], Iman Hajirasouliha [a], Kypros Pilakoutas [a]
[a] Dept. of Civil and Structural Engineering, The University of Sheffield, UK

[*]Corresponding address: Dept. of Civil and Structural Engineering, The University of Sheffield, Sir Frederick Mappin Building, Mappin Street, S1 3JD, Sheffield, UK. T. +44 (0)114 222 5071, F. +44 (0)114 222 5700.
E-mail address: r.garcia@sheffield.ac.uk, reyesgl@gmail.com

ABSTRACT

A full-scale two-storey RC building with poor detailing in the beam-column joints was tested on a shake table as part of the European research project ECOLEADER. After the initial tests which damaged the structure, the frame was strengthened using carbon fibre reinforced materials (CFRPs) and re-tested. This paper investigates analytically the efficiency of the strengthening technique at improving the seismic behaviour of this frame structure. The experimental data from the initial shake table tests are used to calibrate analytical models. To simulate deficient beam-column joints, models of steel-concrete bond-slip and bond-strength degradation under cyclic loading are considered. The analytical models are used to assess the efficiency of the CFRP rehabilitation using a set of medium to strong seismic records. The CFRP strengthening intervention enhanced the behaviour of the substandard beam-column joints, and resulted in substantial improvement of the seismic performance of the damaged RC frame. It is shown that, after the CFRP intervention, the damaged building would experience on average 65% less global damage compared to the original structure if it was subjected to real earthquake excitations.

Keywords: shake table tests; RC frame buildings; CFRP strengthening; nonlinear time-history analyses; seismic performance; inter-storey drift

Nomenclature

f_y	Yield strength of reinforcing steel
f_u	Ultimate strength of reinforcing steel
f_c	Compressive strength of unconfined concrete
E_c	Modulus of elasticity of concrete
f_{FRP}	Tensile strength of FRP composites
E_{FRP}	Modulus of elasticity of FRP composites
θ	Inter-storey drift ratio
f_{cc}^{*}	Compressive strength of confined concrete at ultimate strain
f_{cc}	Compressive strength of unconfined concrete at peak strain
α	Confinement effectiveness factor
ω_w	Volumetric mechanical ratio of confinement with respect to concrete
ε_{cc}^{*}	Ultimate strain of confined concrete
ε_{cc}	Peak strain of unconfined concrete
DI	Global damage index of a frame building
$T_{initial}$	Initial lateral stiffness of a frame
T_{sec}	Secant stiffness at a given roof displacement of a frame

T_{100} Stiffness associated to the roof displacement at the collapse point of a frame

1. Introduction

Much of the existing building stock in Europe, as well as in developing countries, has been designed according to old standards and has little or no seismic provision and often suffers from poor material and construction practices. As a result, many existing buildings have deficient lateral load resistance, insufficient energy dissipation and can rapidly lose their strength during earthquakes, leading to collapse. Extensive human and economical losses in recent major earthquakes (Kashmir, 2005; China, 2008; Indonesia and Italy, 2009; Haiti and Chile, 2010) have highlighted the seismic vulnerability of substandard reinforced concrete (RC) buildings.

The retrofit of seismically deficient structures before earthquakes provides a feasible and cost-effective approach to improving their load carrying capacity and reducing their vulnerability. Over the last decade, the use of externally bonded fibre composite materials (FRPs) has offered engineers a new solution for strengthening seismically deficient buildings [1]. Comparatively to other traditional strengthening techniques, FRP materials possess advantages such as high strength to weight ratio, high resistance to corrosion, excellent durability, ease and speed of in-situ application and flexibility to strengthen selectively only those members that are seismically deficient [2].

Several experimental tests have been conducted to investigate the behaviour of deficient full-scale RC buildings strengthened with FRPs using pseudo-dynamic [3-7] or quasi-static lateral load tests [8]. Based on the results of these experiments, some analytical models were developed to predict the seismic behaviour of deficient and strengthened RC buildings

[9-11]. The results from these studies have confirmed the efficiency of FRP materials at preventing the occurrence of brittle failure modes and improving the seismic behaviour of the strengthened buildings. However, none of the above studies investigated the efficiency of FRPs at improving the seismic behaviour of deficient full-scale RC frames using shaking table tests.

This study investigates experimentally and analytically the efficiency of carbon fibre reinforced materials (CFRPs) to improve the seismic behaviour of substandard RC buildings. This is achieved by using data from shaking table tests on a full-scale one-bay two-storey RC frame with poor detailing in the beam-column joints. The tests were performed on the AZALEE shake table at the Commissariat à l'Énergie Atomique (CEA) Laboratory in Saclay, France, as part of the EU-funded Project ECOLEADER (European Consortium of Laboratories for Earthquake and Dynamic Experimental Research). The main objective of this project was to study experimentally the performance of existing substandard RC frames and different strengthening configurations using CFRPs. The frame was designed and built according to typical old pre-seismic construction practice of southern Europe; hence, it is thought to be representative of substandard buildings typically found in developing countries. Initial shaking table tests were carried out until significant damage was observed. Subsequently, the damaged frame was repaired, and columns and beam-column joints were strengthened using externally bonded CFRPs to perform additional tests. An overview of the ECOLEADER experimental programme is introduced in Section 2 of this paper. Section 3 presents the calibration of analytical models of the bare and CFRP-strengthened frame through nonlinear time-history analyses. In Section 4, the calibrated models are used to investigate the behaviour of the frame in bare, pre-damaged

and CFRP-strengthened conditions subjected to a set of real seismic records. The results from the analyses are compared in terms of capacity to demand ratios, maximum inter-storey drift ratios, roof displacements and global damage indexes. Concluding remarks of this investigation are given in Section 5.

2. Experimental programme

2.1. Geometry of the RC frame, material properties and set-up of tests

The tested building was a one-bay two-storey frame regular in plan and elevation, and was designed with old European earthquake-resistant provisions from the 60's [12]. Consequently, columns and beam-column joints were expected to experience significant damage during the initial shaking tests. The frame was 4.26×4.26 m in plan and had a constant storey height of 3.30 m. A general view of the frame along with details of the general geometry, element sections and corresponding reinforcement are shown in Figure 1. The detailing of the reinforcing steel in beam-column joints is shown in Figure 2. The material properties are obtained based on the average of the results for 12 bar specimens and 24 concrete cylinders. Yield and ultimate strength of steel reinforcement were f_y=551 MPa and f_u=656 MPa, and concrete compressive strength and modulus of elasticity were f_c=20 MPa and E_c=25545 MPa, respectively. The manufacturer specifications of the utilised unidirectional CFRPs were tensile strength f_{FRP}=913 MPa, modulus of elasticity E_{FRP}=105 GPa, and layer thickness of 0.48 mm. An additional mass of 9.0 ton was attached to each slab to simulate real loading conditions as shown in Figure 1b.

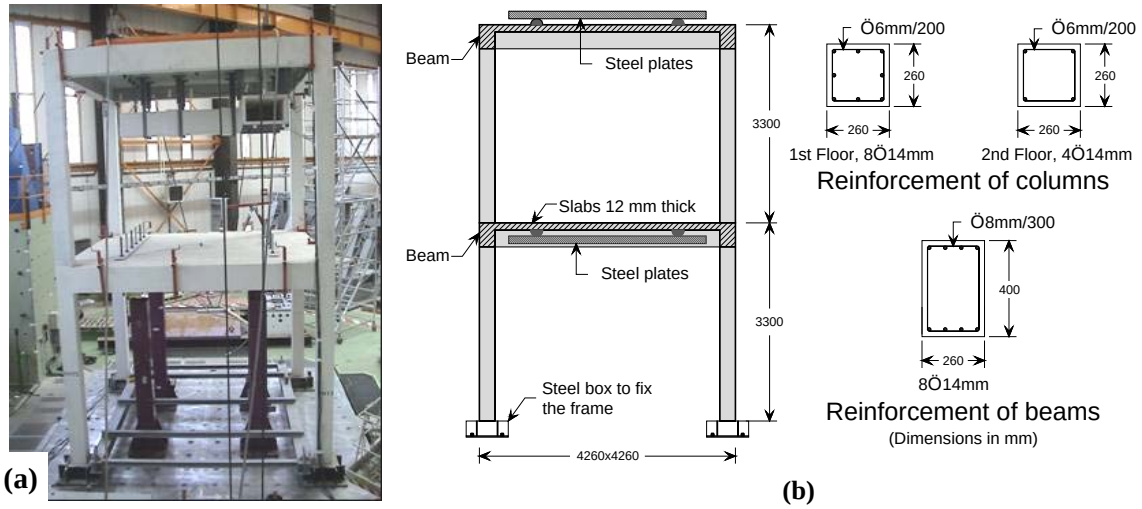

Figure 1. (a) General view (from reference [12]) and (b) geometry of the frame and structural elements.

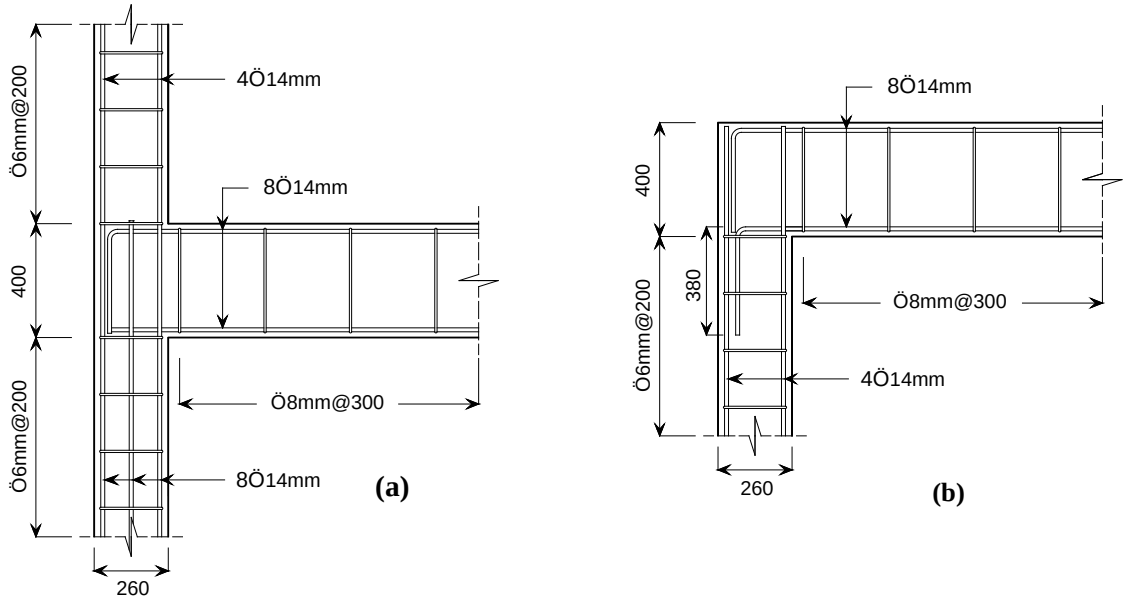

Figure 2. Detailing of reinforcing steel in beam-column joints at (a) 1st storey and (b) 2nd storey.

The structure was instrumented with displacement and acceleration transducers at each storey to monitor the response history during the shaking tests. The displacement transducers were attached to an external rigid frame to facilitate the measurements and quantify the residual displacements after each test. Full details of the experimental work can be found in [12]. In this paper, the inter-storey drifts and displacements from the experimental tests are used to calibrate the nonlinear analytical models using DRAIN-3DX software [13].

2.2. Tests on the Bare and CFRP-strengthened Structure

The experimental programme consisted of unidirectional horizontal input shaking using increasing peak ground accelerations (PGA) levels ranging from 0.05g to 0.4g. A single ground motion record was used based on the Eurocode 8 (EC8) soil profile type C spectrum [14]. Natural frequencies of the structure were obtained using white noise as input signal before the start and after each test. For this purpose, a low intensity excitation containing a frequency range of 0.5-50 Hz was used. The accelerations recorded at the base and at each storey were then post-processed to identify the natural frequencies of the first two modes of vibration.

After the initial series of tests, the damaged frame (see Figure 11) was strengthened locally with externally bonded CFRP composites using a wet lay-up technique. The main purpose of the rehabilitation was to produce a beam mechanism, which is in line with modern seismic design philosophy. Before the strengthening intervention, the damaged concrete was repaired using repair mortar and the main cracks injected with epoxy resin. Concrete surfaces at the application zones were smoothed and prepared to improve the adherence between the existing concrete and the fibre sheets. One vertical CFRP sheet (parallel to the

columns axes) was attached at the interior and exterior faces of columns ends to enhance their flexure strength (Figure 3a). Beam-column joints at both storeys were also strengthened using one orthogonal sheet to avoid a premature shear failure, as shown in Figure 3b. Two thin strips of CFRPs were wrapped around the beams ends to prevent premature debonding of the sheets applied to strengthen the joints (Figure 3b). Additionally, it was decided to use CFRP confinement to increase further the column capacity and avoid possible buckling and premature debonding of the longitudinal sheets along the columns axes (Figure 4). The existing transverse reinforcement was sufficient to prevent shear failure in beams and columns; therefore, no additional FRP was required to prevent this type of failure. Further details of the rehabilitation strategy and the damage sustained by the bare and strengthened frames are reported in [12,15,16].

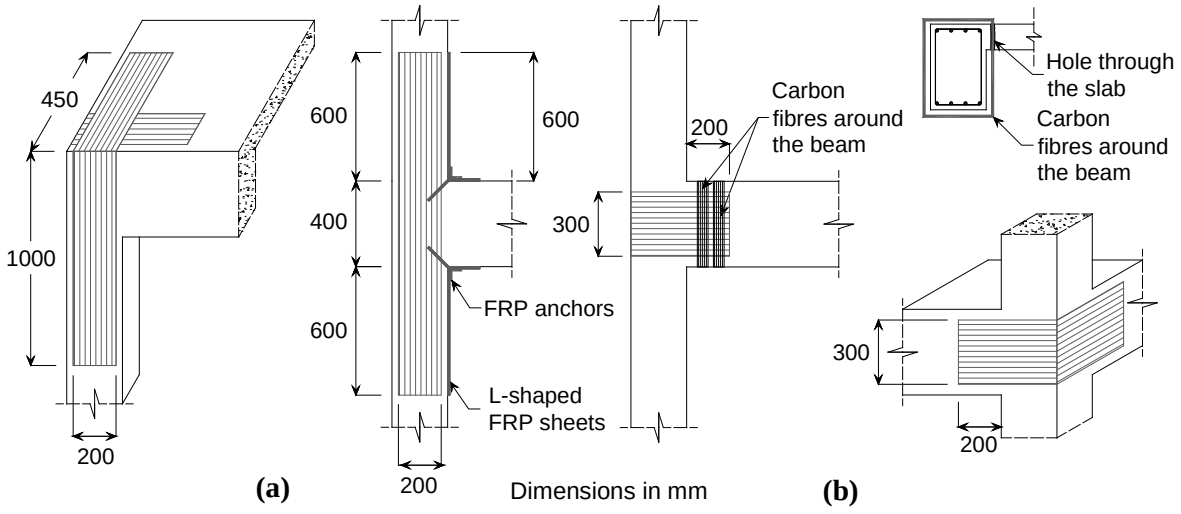

Figure 3. Rehabilitation of the frame using CFRPs at (a) exterior faces of columns, and (b) exterior zone of beam-column joints.

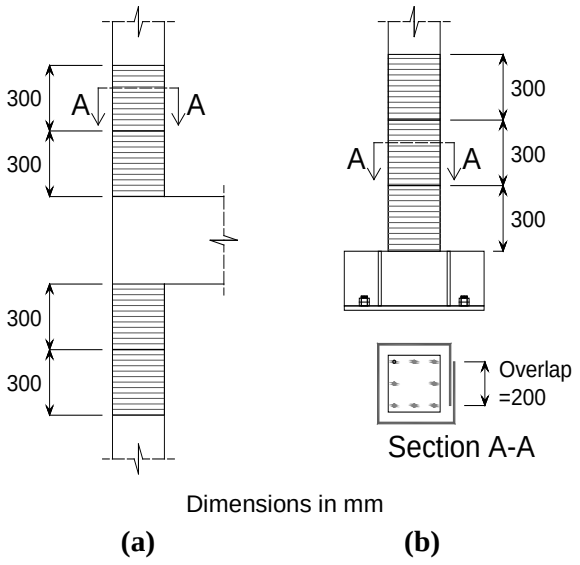

Figure 4. Confinement of the columns using CFRPs at (a) columns ends, and (b) bottom of 1st storey columns.

Following the CFRP-strengthening of the frame (Figure 5a), a second series of shaking table tests were conducted with PGA levels ranging from 0.05g to 0.5g. No evident damage appeared during the test at PGA= 0.05g. A visual inspection detected the first damage at the CFRP sheets at the 2nd storey columns after the tests at PGA level of 0.2g. No further damage was observed at columns or CFRP sheets until after the final tests, however, some fracture of the sheets occurred at beam-column joints. The adopted strengthening strategy was effective at preventing debonding of the CFRP sheets as this type of failure was not observed during the tests. However, after the tests at a PGA of 0.5g, significant cracking occurred at the beams ends, as shown in Figure 5b. Figure 6 shows the deformed shape at maximum deformation for the frame in bare and CFRP-strengthened conditions.

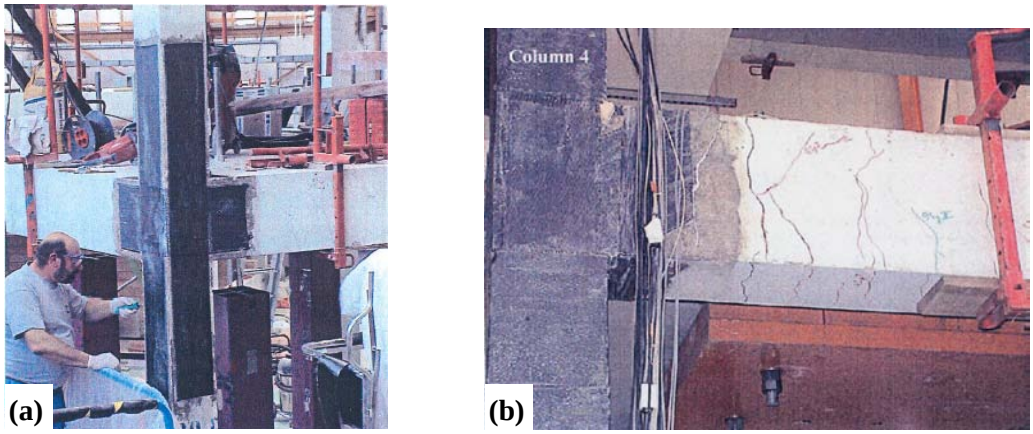

Figure 5. (a) CFRP-strengthening of the frame and (b) damage at beam ends after the tests on the strengthened frame [12].

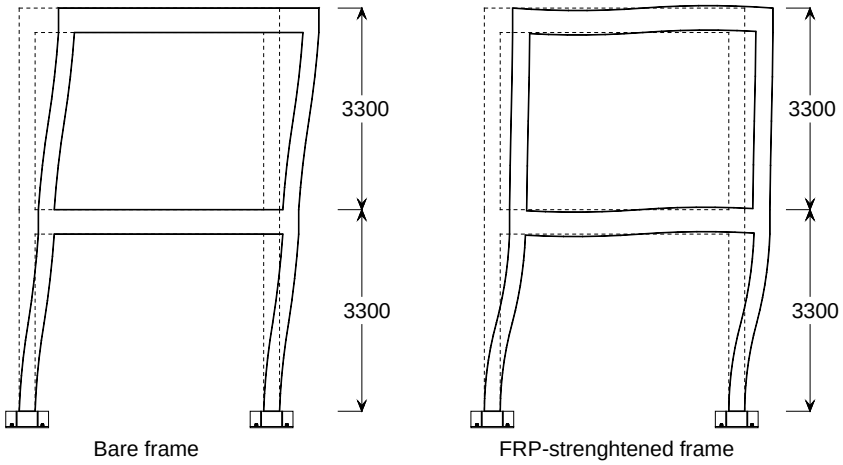

Figure 6. Deformed shape for the frame in bare and CFRP-strengthened conditions at PGA=0.4g.

3. Analytical modelling

3.1. Modelling of the bare and CFRP-strengthened frame in DRAIN-3DX

Numerical models were developed in DRAIN-3DX [13], which is a software widely used by many researchers to evaluate the seismic performance of building structures. Because of the symmetry in plan, the frame was modelled in 2D for computational efficiency (Figure 7a). Beams and columns were modelled using a fibre element (Element Type 15) of

distributed plasticity [17]. To increase the accuracy of the analysis, each section consisted of discrete steel and concrete fibres as shown in Figure 7b. The steel reinforcement and concrete characteristics were based on the constitutive models given in Eurocode 2 [18]. Vertical nodal loads were assigned along the beams to simulate the distributed dead load from slabs and beams. Additional nodes added at the top and bottom of the outermost column elements simulated the actual geometry of columns and beam-column joints. The masses at each storey were lumped at the two corresponding exterior nodes and calculated assuming a concrete density equal to 24 kN/m^3. Elastic damping was introduced using a stiffness and mass proportional Rayleigh damping model [19]. Appropriate damping values (2 to 5%) were assigned to the first and second modes of vibration to achieve the best agreement with the experimental results. Second order (P-Δ) effects were also included in the analysis.

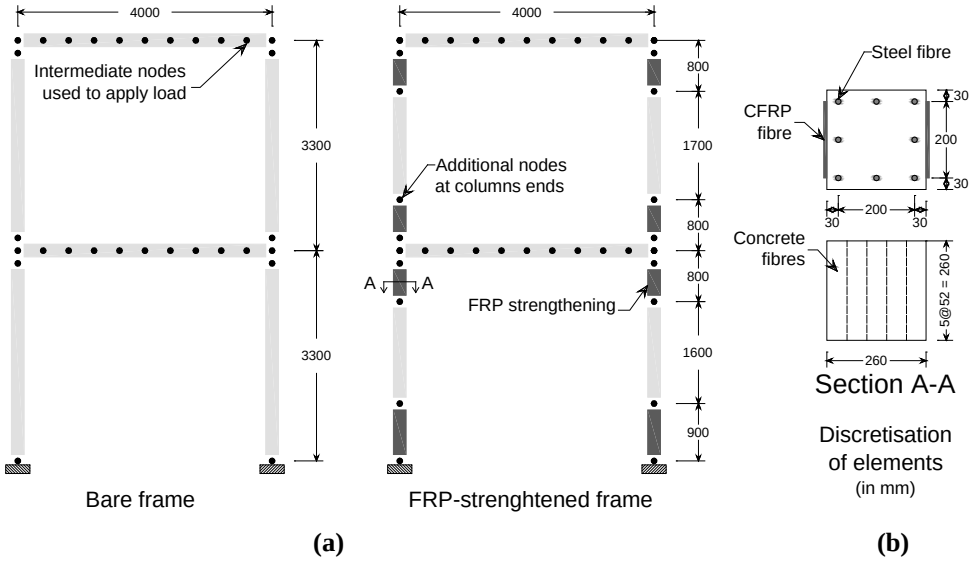

Figure 7. (a) Analytical models of bare and strengthened frames, and (b) fibre elements used in DRAIN-3DX.

Previous research showed the need of considering the additional deformations generated by stiffness degradation and slippage of the reinforcing bars to predict the actual seismic behaviour of existing RC frames [20]. Damage accumulation was included in the analyses by considering a stiffness degradation factor in the stress-strain relationship of concrete. To consider bar slippage, additional deformations occurring at the joints were specified using zero-length connection hinges at column ends. The fibre properties used for the elements were chosen to model bond stress-bar slip within the beam-column joints, and included stiffness and strength degradation factors. Partial degradation was initially assigned to both bond-stiffness and bond-strength [17]. Gap properties in compression were considered at the connection face to simulate crack opening according to the recommendations in [17]. Figure 8 shows the constitutive models of concrete, bond-slip and gap properties used for the nonlinear time-history analyses.

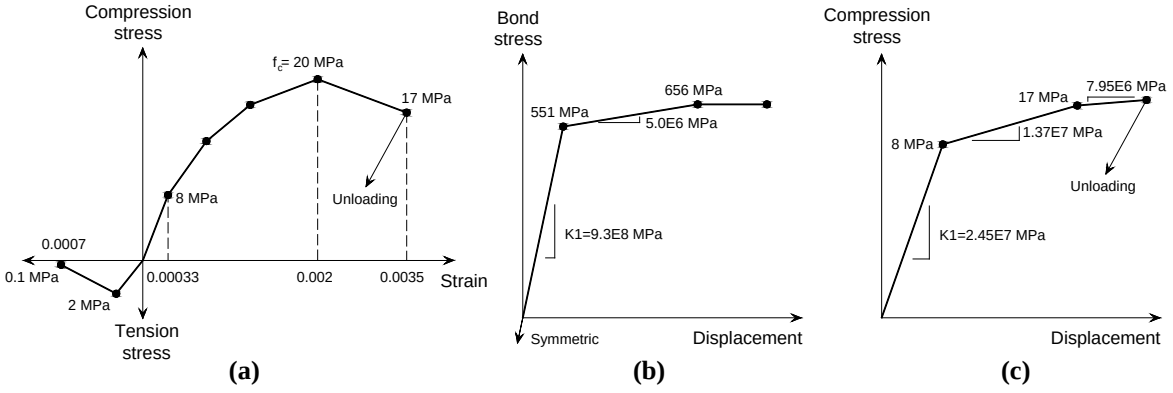

Figure 8. Constitutive models of (a) concrete, (b) bond-slip, and (c) gap properties used for the analyses (adapted from [17]).

In order to model the strengthened frame, additional nodes were added to define the CFRP-confined zones of columns. The effect of the strengthening was introduced using the

design-oriented constitutive model for FRP-confined concrete proposed by Mortazavi [21,22], according to Eqs.(1) and (2):

$$\frac{f_{cc}^{*}}{f_{cc}} = 1 + 1.7(\alpha\omega_{w})^{0.8} \tag{1}$$

$$\varepsilon_{cc}^{*} = \varepsilon_{cc}\left(1 + 6.7\left(\frac{f_{cc}^{*}}{f_{cc}} - 1\right)^{2/3}\right) \tag{2}$$

where f_{cc}^{*} and f_{cc} are the concrete compressive strength in confined and unconfined conditions, respectively; α is the confinement effectiveness factor; ω_w is the volumetric mechanical ratio of the confinement with respect to the concrete, and ε_{cc}^{*} and ε_{cc} are the confined ultimate strain and unconfined peak strain of concrete, respectively.

Although several FRP confinement models currently exist, Mortazavi's model was adopted mainly due to its simplicity and good agreement with previous experimental data [21]. In this work, the effectiveness confinement factor α [used in Eq. (1)] for the square column sections was calculated using the recommendations by *fib* Bulletin 14 [23]. The computed ultimate compression strength and ultimate strain used for the analysis were f_{cc}^{*} = 30 MPa and ε_{cc}^{*} = 0.010, respectively. The vertical CFRP sheets at column ends and joints were represented using finite fibre elements located at the column faces (Figure 7b). The fibres were assumed to have elastic behaviour until failure and modelled with the mechanical characteristics supplied by the manufacturer. The analytical model disregarded possible debonding of the FRP sheets as this type of failure was not observed during the experimental tests.

3.2. Calibration of the analytical models

The experimental data from the shake table tests were used to calibrate the analytical models of the bare frames developed in DRAIN-3DX. Appropriate values for degradation factor and damping ratios were assigned to have the best agreement between analytical and experimental results. Final values of the parameters used for the calibration of the analytical models are presented in Table 1.Natural frequencies obtained from white noise tests are compared with the analytical results in Table 2. The results show that, for the first two modes of vibration, the dynamic properties of the bare frame are well captured by the analytical models.

The experimental and analytical displacement histories of the bare frame are compared in Figures 9 and 10 for PGA levels of 0.05, 0.2 and 0.4g. In spite of some differences, the results indicate that the predicted and measured displacements compare reasonably well along the entire time duration of the excitation. It should be mentioned that in Figure 10 at a PGA level of 0.4g, the experimental response of the 2^{nd} storey is only shown until 28.0 s due to failure of the displacement transducer. Inter-storey drift calculations (see Table 3) shows that the two storeys have similar inter-storey drifts at low to medium excitation levels (PGA of 0.05 to 0.2g), however, inter-storey drift at the second floor increases considerably as the excitation level increases to 0.4g. This can be attributed to damage at the 2^{nd} storey beam-column joints, as observed during the experiments (Figure 11b).

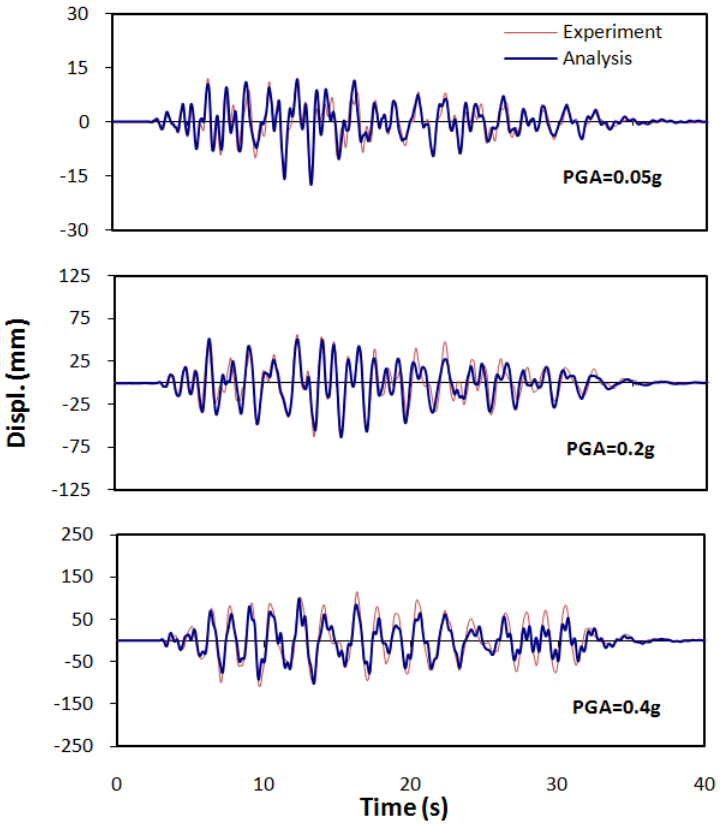

Figure 9. Displacement histories from experiments and analysis for 1st storey at PGA levels of 0.05, 0.2 and 0.4g, bare frame

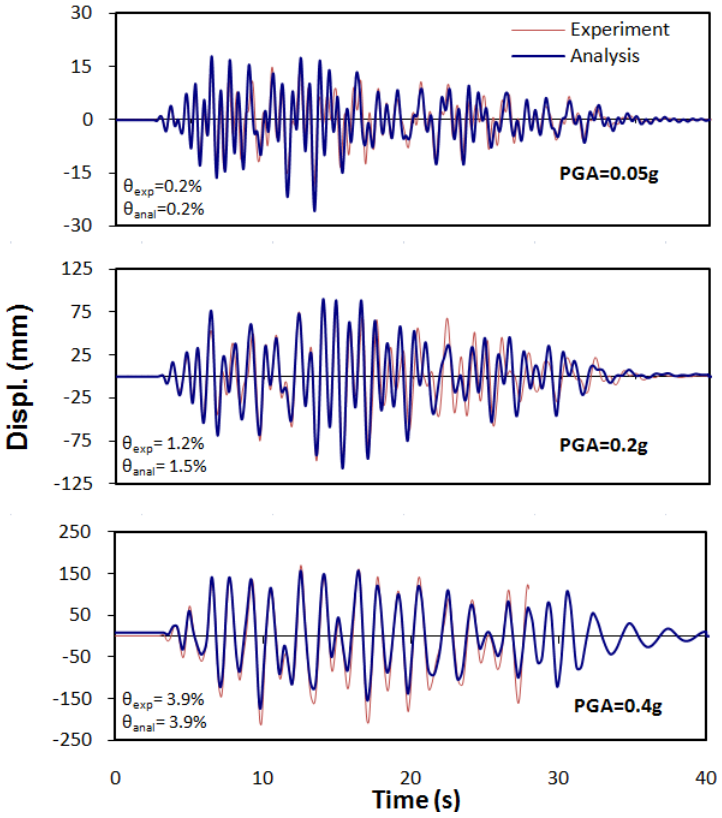

Figure 10. Displacement histories from experiments and analysis for 2nd storey at PGA levels of 0.05, 0.2 and 0.4g, bare frame

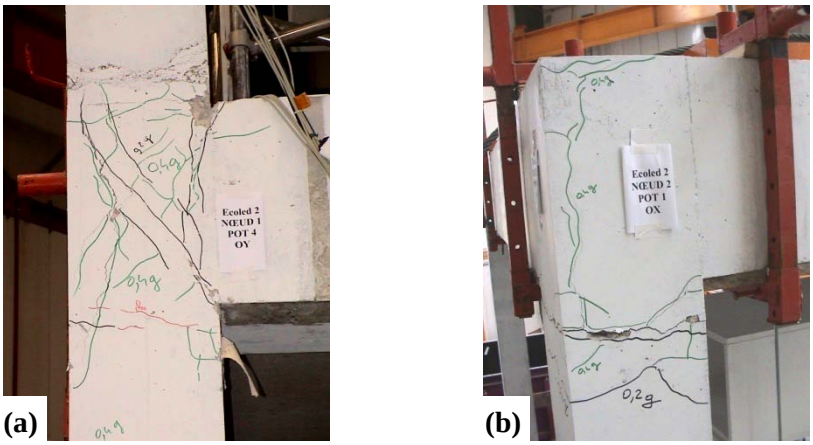

Figure 11. Damage after the test on bare frame at a PGA level of 0.4g in beam-column joints of (a) 1st storey, and (b) 2nd storey

The calibrated model of the bare frame was used to develop the analytical model of the strengthened frame in DRAIN-3DX, as explained in Section 3.1. In the strengthened model, bond stress-bar slip within the beam-column joints was not considered as the frame was repaired with resin injection and additional confinement was provided by the CFRP. It is shown in Table 2 that the analytical model of the strengthened frame was capable of predicting the period of the first two modes of vibration with good accuracy. The results indicate that the epoxy-injection of cracks and the strengthening strategy were effective at restoring the dynamic characteristics of the frame, as after the strengthening intervention the period of the damaged frame was decreased and was close to the period of the post-cracked elastic stage.

Table 2 also shows that whilst the structural periods of the bare and strengthened frame were very similar at the PGA level of 0.2g, inter-storey drifts were controlled better in the top floor of the strengthened structure using CFRP. This suggests that the bare frame experienced some structural deterioration at that excitation level, especially at the top floor joints as shown in Figure 11b. Data from strain gauges confirms that such deterioration could be attributed to bond-slip prior to yielding of the column reinforcing steel. The local CFRP intervention at joints and columns delayed the degradation due to bond-slip of the reinforcement at this and higher PGA levels and contributed to the better control of top floor deformations.

Figures 12 and 13 compare the experimental and analytical displacement histories of the CFRP-strengthened frame for PGA levels of 0.05, 0.2 and 0.4g. It is shown that the analytical results compare well with the measured displacements for different PGA levels.

This implies that it is possible to develop appropriate analytical models to predict the behaviour of the CFRP-strengthened frame with an acceptable accuracy.

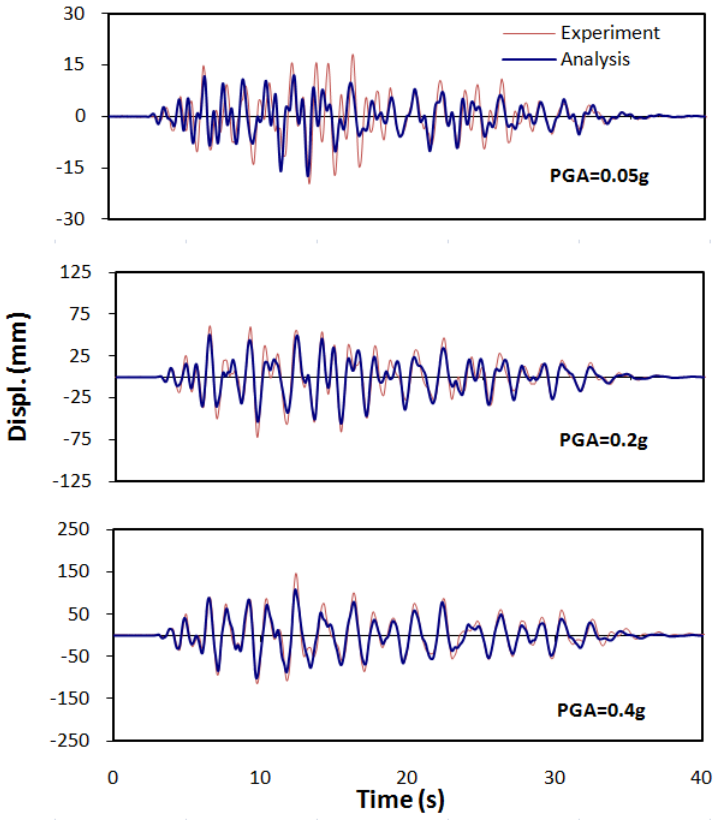

Figure 12. Displacement histories from experiments and analysis for 1st storey at PGA levels of 0.05, 0.2 and 0.4g, CFRP-strengthened frame

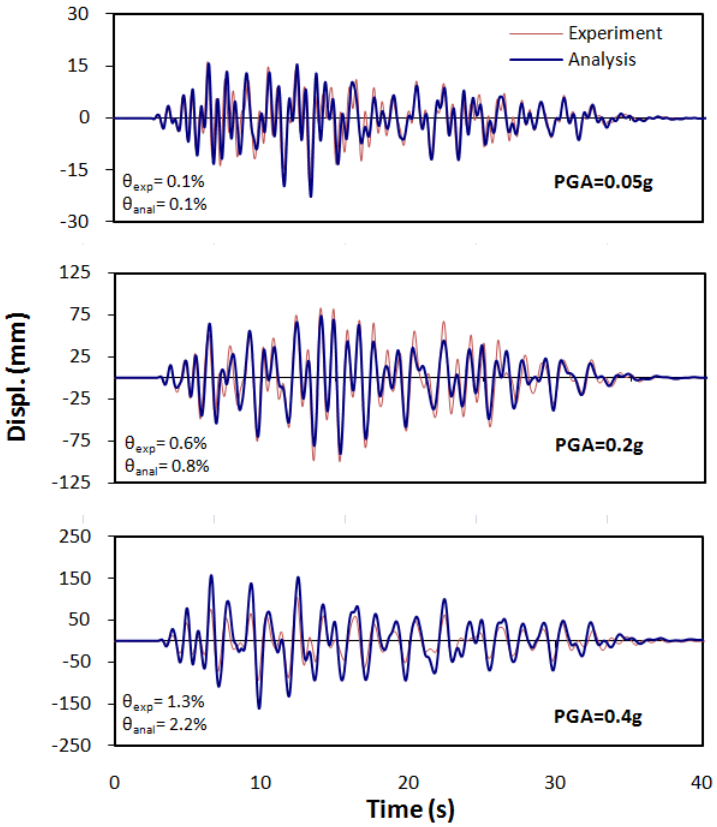

Figure 13. Displacement histories from experiments and analysis for 2nd storey at PGA levels of 0.05, 0.2 and 0.4g, CFRP-strengthened frame

Table 3 compares the maximum inter-storey drift ratios obtained from the experimental tests and analytical models for different PGA levels. Based on the results, it can be concluded that the analytical models of both bare and strengthened frame provide a reasonable estimate of the maximum inter-storey drifts for earthquake excitations with different PGA levels. However, in general terms, the analytical models for both bare and strengthened structures tends to slightly underestimate the inter-storey drift for the 1st storey, while the inter-storey drift response for the 2nd storey is slightly overestimated. The results indicate that the application of CFRPs significantly decreased the 2nd inter-storey drift, while it slightly increased the 1st inter-storey drifts. This is attributed to the fact that the rehabilitation strategy changed the behaviour of the bare frame by preventing extensive

damage and possible failure of the beam-column joints at the first storey. Design guidelines such as FEMA 356 [24] place limits on acceptable values of inter-storey drift ratios implying that exceeding these limits is a violation of a performance objective. According to FEMA 356, maximum inter-storey drifts of 1%, 2% and 4% correspond to Immediate Occupancy (IO), Life Safety (LS), and Collapse Prevention (CP) performance levels, respectively. Most of the current seismic design guidelines aim to limit the structural and non-structural damage to the LS performance level during the design earthquake. The results indicate that by using CFRP strengthening, the maximum inter-storey drift of both floors of the damaged building was reduced from 3.9% (near to the theoretical collapse) to 2.5% (closer to LS). This implies that the damaged building after strengthening was capable of resisting the design earthquake even under strong seismic excitations.

4. Frame performance using real earthquake records

In order to investigate the efficiency of the CFRP strengthening under real seismic excitations, the frame analytical models were subjected to a set of real seismic records as listed in Table 4 [25]. These excitations correspond to sites having a soil profile similar to EC8 soil type C; therefore, they are expected to have similar frequency content (Figure 14). The selected seismic records have PGA values ranging from 0.24 to 0.51g, representing moderate to strong earthquakes. The use of earthquake records having different levels of input energy allows assessing quantitatively the expected structural damage. Real earthquake records were used for this evaluation rather than artificial ones, as the latter appear to be more onerous for the seismic assessment of existing buildings [26].

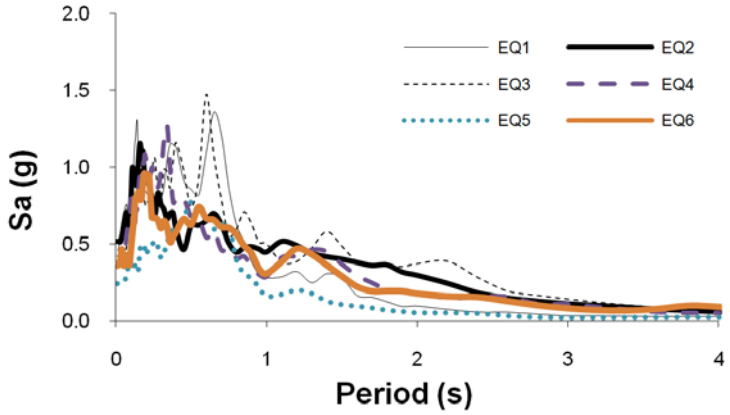

Figure 14. Response spectra of the real earthquake records used in the evaluation (5% damping).

The efficiency of the rehabilitation strategy is investigated by exploring the expected structural and non-structural damage experienced by the frame models in three different conditions: (i) Bare frame: the original frame before applying seismic excitation; (ii) Damaged frame: the bare frame after it was subjected to the maximum shaking table input level of 0.4g (before strengthening); and (iii) CFRP-strengthened frame: the damaged frame after the strengthening intervention.

4.1. Demand to capacity ratios for curvature ductility

Demand to capacity (D/C) ratios for curvature ductility, $(D/C)_{\mu k}$, are used as an appropriate performance criterion for the seismic assessment of structural elements of existing buildings [27]. Figure 15 compares $(D/C)_{\mu k}$ of the columns for the set of real earthquakes under the different conditions described above. It should be noted that $(D/C)_{\mu k}$ is an indicator of expected local damage in the columns. The capacities of the columns were computed using conventional section analysis and include the effect of gravity and seismic axial loads. The results show that D/C ratios of the CFRP-confined columns are significantly lower than those of the bare and damaged models by a factor ranging from 3

to 4. Consequently, compared to the original and damaged bare frame, less structural damage is expected in the columns of the CFRP-strengthened frame during earthquake excitations. As shown in Figure 15, whilst in the bare frame the $(D/C)_{\mu k}$ ratios of the 1st and 2nd storey columns differ significantly, they are relatively closer for the CFRP-strengthened structure. This confirms that the design of the bare structure was inadequate for these earthquakes and would lead to extensive damage in the 1st floor before the capacity of the columns at the 2nd floor was fully utilised. The strengthening intervention resulted in a better use of material capacity as the $(D/C)_{\mu k}$ ratios of the columns are more uniform over the frame height.

It should be mentioned that the brittle joint failure mechanism in the damaged building prevents the full exploitation of the available curvature ductility of the columns. However, for the strengthened building, brittle failures are prevented and the full capacity and ductility of the columns could be utilised if there is sufficient demand.

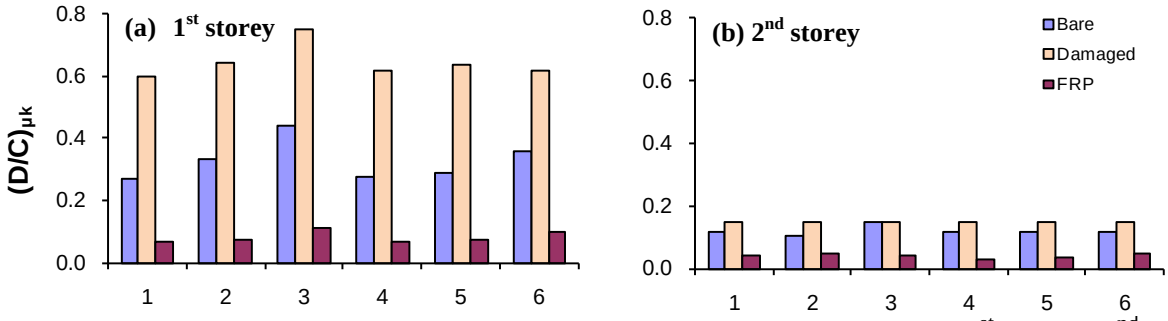

Figure 15. Demand to capacity ratios (D/C) for curvature ductility for (a) 1st and (b) 2nd storey columns in bare, damaged and CFRP-strengthened conditions, six real earthquakes

4.2. Maximum response displacements

To evaluate the structural and non-structural damage experienced by the bare, damaged and CFRP-strengthened models, maximum response displacement parameters are also examined. Figure 16 compares the maximum roof (top) displacement demands of the

model for the set of six real earthquake excitations. It is shown that the maximum roof displacement is very similar for the bare and CFRP-strengthened models. This is in line with the strengthening objectives, as the local intervention with CFRP materials aimed at increasing the strength capacity of columns and beam-column joints, without modifying significantly the original stiffness characteristics of the frame. Comparatively, the theoretical roof displacements of the strengthened frame are 20 to 45% less than those of the damaged frame.

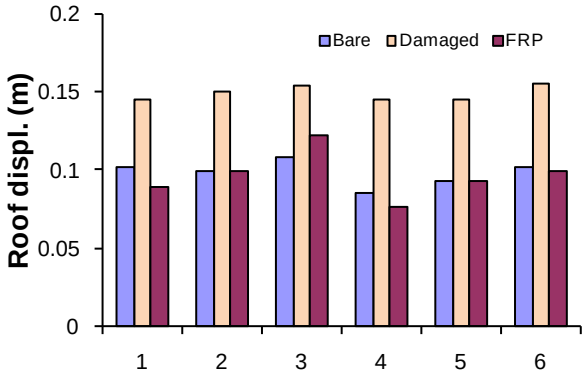

Figure 16. Maximum roof displacement of frames in bare, damaged and CFRP-strengthened conditions, six real earthquakes

Maximum roof displacements provide an insight into the global behaviour of an existing structure. However, inter-storey drift ratios are considered a more reliable indicator of damage to non-structural elements and are widely used as a failure criterion, as suggested by FEMA 356. Therefore, the efficiency of the strengthening technique is examined in terms of maximum inter-storey drifts. Maximum inter-storey drift ratios of the bare, damaged and CFRP-strengthened frame models are given in Figure 17 for the set of six seismic records. Larger inter-storey drift ratios at the 2nd floor of the bare frame are due to the significant damage at the 2nd storey beam-column joints. The results indicate that the strengthening strategy was successful at reducing the damage at beam-column joints, which

resulted in a smaller inter-storey drift at the 2nd floor. This is evident in particular for the stronger energy input records (EQ 1 and 3), where the strengthened frame experienced, on average, 35% less inter-storey drift compared to the bare frame. The efficiency of the strengthening strategy is emphasised by comparing the maximum inter-storey drift of the damaged and CFRP-strengthened models. While the maximum inter-storey drifts ratios of the 2nd storey for the damaged condition were near or exceeded a value of 4% (i.e., CP performance level), those of the strengthened models are always between 1 to 2%. However, the maximum inter-storey drift ratio of the 1st storey is slightly higher in the strengthened structure. These results are in agreement with those from the experimental tests (see Table 3), where the inter-storey drifts for the 1st and 2nd storeys decreased and increased, respectively, after the application of CFRP composites. Maximum inter-storey drift ratios of the 2nd storey of the damaged frames were decreased by up to 75% after the strengthening intervention.

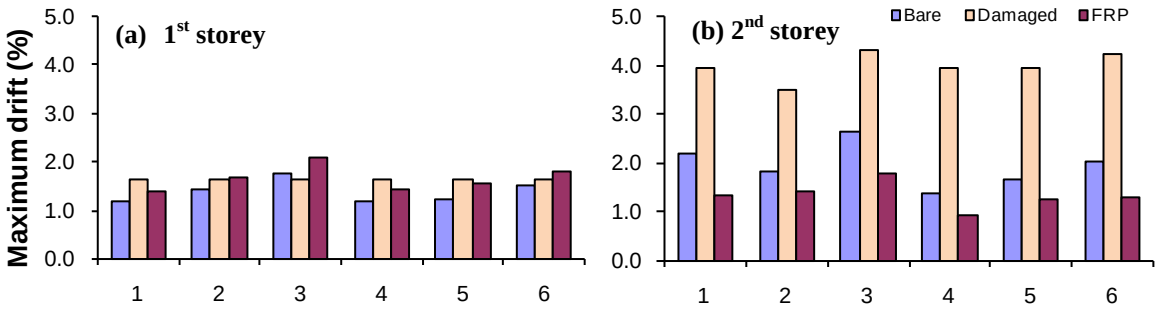

Figure 17. Maximum inter-storey drift ratios for (a) 1st and (b) 2nd storeys of frames in bare, damaged and CFRP-strengthened conditions, six real earthquakes

4.3. Performance levels and global damage

Table 5 summarises the seismic performance levels of the bare, damaged and CFRP-strengthened frame models for the six selected seismic records. The results indicate that, whilst the performance of the bare frame exceeded the LS level in three of the selected earthquakes (EQ 1, 3 and 6), the performance of the strengthened frame was always within the LS level. Table 5 shows that, as expected, the performance of the damaged frame always reached or exceeded the CP level for the selected medium to strong earthquakes. It can be concluded that the strengthening method improved adequately the seismic performance of the deficient frame, and no severe structural damage is expected to occur in the CFRP-strengthened models when subjected to the selected real earthquakes.

It has been suggested that inter-storey drift alone may not be necessarily the best performance parameter to assess global damage, and that lateral stiffness is a more reliable measure of the likely damage to be experienced by a building [28]. Hence, recent studies have proposed to relate building damage with a change in the dynamic properties of RC frame buildings [28,29]. Based on this approach, the following equation can be used to relate damage of an RC frame at a given roof displacement as a function of its structural period at damage condition state (i.e. stiffness) [20]:

$$DI = 100 \cdot \left(\frac{T_{sec} - T_{initial}}{T_{100} - T_{initial}} \right) \tag{3}$$

where DI is the global damage index of the frame structure, $T_{initial}$ is the initial stiffness of the frame, T_{sec} is the secant stiffness at a given roof displacement, and T_{100} the stiffness associated to the roof displacement at the collapse point of the frame (see definitions in Figure 18). In Eq. (3), a DI value of zero implies no damage to the building, whereas a DI

value of 100 or larger represents the theoretical collapse of the building. In the context of this research, Eq. (3) was used to predict the global damage level of the frame models under the real selected earthquakes. This was done by considering the initial period, $T_{initial}$, obtained from a pushover analysis on the frame in bare, damaged and CFRP-strengthened conditions. To achieve this, a lateral "modal" pushover load pattern was used according to EC8. T_{sec} was defined as the period of the frame at the maximum roof displacement recorded during the nonlinear time-history analyses for the real seismic records (see Figure 18). The ultimate condition of the frame corresponding to theoretical collapse (T_{100}) was assumed to be equal to the roof displacement at which the columns exceeded a pre-established acceptance criterion. For this purpose, the plastic rotation corresponding to the CP performance level given by FEMA 356 was adopted, and used to define the theoretical collapse of the frames.

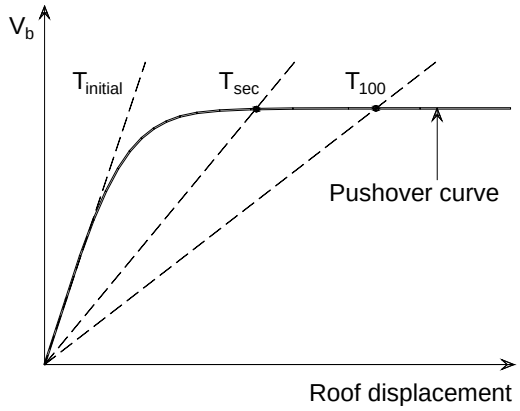

Figure 18. Definition of initial, secant and ultimate roof displacements used to calculate global damage indexes (*DIs*)

Figure 19 compares the corresponding *DIs* of the bare, damaged and strengthened models subjected to the six selected earthquakes. It is shown that the damaged frame had limited capacity to resist a new earthquake, as it practically reached or exceeded the theoretical

collapse for all the seismic records. The results indicate that the global damage experienced by the CFRP-strengthened frame was, on average, 65% less compared to the bare frame. Based on the results, it can be concluded that the seismic behaviour of the damaged frame was significantly enhanced after implementing the rehabilitation strategy. It is estimated that, for practical applications, the rehabilitation costs of adopting such a strategy are likely to be in the range of 5-15% of the cost of the building. This estimate is based on the authors' experience of costs of rehabilitation of buildings in the Mediterranean region and can vary significantly depending on labour costs and location of the building. Such costs are clearly justified in the case of the damaged building, but they are not necessarily justified for the given earthquakes which for a new structure have a probability of less than 10% of affecting the structure over its lifetime. However, if the structure is in need of modernisation, then the costs of rehabilitation can be reduced and the justification for rehabilitation becomes stronger.

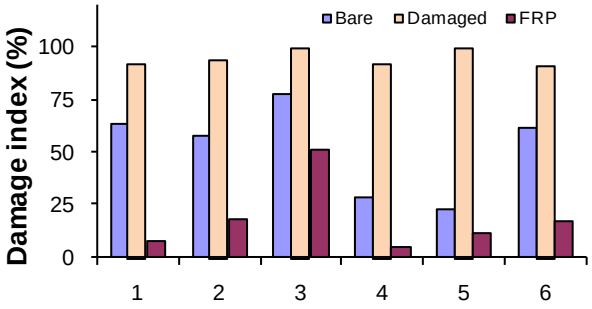

Figure 19. Damage indexes (*DIs*) of frames in bare, damaged and CFRP-strengthened conditions, six real earthquakes

5. Conclusions

This paper investigated experimentally and analytically the efficiency of externally bonded carbon fibre composite materials (CFRPs) in improving the behaviour of a seismically

deficient full-scale two-storey RC frame. The frame was tested on a shake table as part of the EU-funded ECOLEADER Project. From the experimental and analytical results, the following conclusions are drawn:

1. The results of the shaking table test demonstrated that the adopted local strengthening strategy using CFRP materials was effective at changing the plastic hinge mechanism from column-sway to beam-sway, which is in line with modern seismic design philosophy. The epoxy-injection of cracks and the adopted strengthening strategy were also effective at restoring the initial dynamic characteristics of the RC frame.

2. Analytical models were calibrated using the experimental results of the bare and strengthened frames. The analytical models provided a reasonable estimate of the displacement demands for earthquake excitations with different PGA levels.

3. The efficiency of the rehabilitation strategy was further investigated analytically using a set of six real earthquake records. By computing demand to capacity ratios, it is shown that the use of CFRP materials increases significantly the deformability capacity of the columns, hence reducing the expected local structural damage when the beam-column joint failure is prevented.

4. The use of CFRP composites resulted in a considerable reduction of inter-storey drift at the second floor since it delayed the deterioration of the building due to bond-slip of the column reinforcing steel. Consequently, the seismic performance of the bare frame was improved from Collapse Prevention to Life Safety performance level for the simulated and medium to strong earthquake records used in this study.

5. The results indicate that, for the set of selected records, the strengthened building experienced on average 65% less global damage compared to the original building.

6. The cost of strengthening is justified for the damaged structure but may be too expensive as a preventive measure.

Acknowledgments

The first author acknowledges the financial support provided by the National Council of Science and Technology (CONACYT-Mexico) and DGRI-SEP through its Complementary Scholarship programme. The second author wishes to acknowledge the financial support provided by the EU through the Marie Curie International Incoming Fellowship.

References

[1] Pendhari SS, Kant T, Desai YM. Application of polymer composites in civil construction: a general review. Comp Struct 2008; 84(2): 114-24.

[2] Gdoutos EE, Pilakoutas K, Rodopoulos CA. Failure analysis of industrial composite materials. 1st ed. New York: McGraw-Hill; 2000.

[3] Pinto AV, Verzeletti G, Molina J, Varum H, Pinho R, Coelho E. Pseudodynamic tests on non-seismic resisting RC frames (bare and selective retrofit frames). Report EUR 20244, JRC-IPSC, Ispra, Italy; 2002.

[4] Balsamo A, Colombo A, Manfredi G, Negro P, Prota A. Seismic behavior of a full-scale RC frame repaired using CFRP laminates. Eng Struct 2005; 27(5): 769-80.

[5] Balsamo A, Manfredi G, E M, Negro P, Prota A. Seismic rehabilitation of a full-scale structure using GFRP laminates. ACI Struc J, SP230-75. 2005: 1325-44.

[6] Di Ludovico M, Manfredi G, Mola E, Negro P, Prota A. Seismic behavior of a full-scale RC structure retrofitted using GFRP laminates. J Struct Eng 2008; 135(5): 810-21.

[7] Di Ludovico M, Prota A, Manfredi G, Cosenza E. Seismic strengthening of an under-designed RC structure with FRP. Earthq Eng Struct Dyn 2008; 37(1): 141-62.

[8] Della Corte G, Barecchia E, Mazzolani FM. Seismic upgrading of RC buildings by FRP: full-scale tests of a real structure. J Mater Civ Eng 2006; 18(5): 659-69.

[9] Jeong SH, Elnashai AS. Analytical assessment of an irregular RC full scale 3D test structure. Mid-America Earthquake Center, Dept. of Civil and Environmental Engineering, University of Illinois at Urbana-Champaign, Urbana, Illinois, USA; 2004, p. 146.

[10] Kosmopoulos AJ, Fardis MN. Estimation of inelastic seismic deformations in asymmetric multistorey RC buildings. Earthq Eng Struct Dyn 2007; 36(9): 1209-34.

[11] Galicia HI, Jara JM, Negro P. Strengthening of a four-story building model using CFRP fabrics. In Proc. of the 8th International Symposium on Fiber-Reinforced Polymer Reinforcement for Concrete Structures (FRPRCS8); 2007; Patras, Greece.

[12] Chaudat T, Garnier C, Cvejic S, Poupin S, Le Corre M, Mahe M. ECOLEADER Project No. 2: Seismic tests on a reinforced concrete bare frame with FRP retrofitting - Tests Report. SEMT/EMSI/RT/05-006/A, CEA, Saclay, France; 2005.

[13] Prakash V, Powell GH, Campbell S. Drain-3DX: Base program description and user guide. SEEM Report 94/07, University of California-Berkeley, USA; 1994.

[14] CEN. Eurocode 8. Design of Structures for Earthquake Resistance Part 1: General rules, seismic actions and rules for buildings. Comité Européen de Normalisation, Brussels, Belgium; 2004.

[15] Chaudat T, Pilakoutas K, Papastergiou P, Ciupala MA. Shaking table tests on reinforced concrete retrofitted frame with carbon fibre reinforced polymers (CFRP). In In Proc. of the 1st European Conference on Earthquake Engineering and Seismology; 2006; Geneva, Switzerland.

[16] Papastergiou P, Pilakoutas K, Ciupala MA, Chaudat T. Enhancement of RC column and joint resistance by using CFRP strengthening. In Halliwell S, Whysall C, editors. In Proc. of the 4th International Conference in Advanced Composites in Construction (ACIC 2009); 2009; Edinburgh, Scotland. p. 559-69.

[17] Powell GH, Campbell S. Drain-3DX: Element description and user guide for element Type01, Type04, Type05, Type08, Type09, Type15, and Type17. SEEM Report 94/08, University of California-Berkeley, USA; 1994.

[18] CEN. Eurocode 2. Design of concrete structures Part 1-1: General rules and rules for buildings. Comité Européen de Normalisation, Brussels, Belgium; 2004.

[19] Chopra AK. Dynamics of structures: theory and applications to earthquake engineering. 2nd ed. Upper Saddle River, NJ: Prentice-Hall; 2001.

[20] Kyriakides N. Vulnerability of RC buildings and risk assessment for Cyprus. PhD Thesis, Dept. of Civil and Structural Engineering, University of Sheffield, UK. 2007.

[21] Mortazavi A. Behaviour of confined concrete columns with and without lateral pre-tensioning. PhD Thesis, Dept. of Civil and Structural Engineering, University of Sheffield, UK. 2003.

[22] Ciupala MA, Pilakoutas K, Mortazavi AA. Utilisation of FRP composites in the confinement of concrete. In Proc. of the 8th International Symposium on Fiber-Reinforced Polymer Reinforcement for Concrete Structures (FRPRCS8); 2007; Patras, Greece.

[23] *fib* Bulletin 14. Externally bonded FRP reinforcement for RC structures. CEB-FIP, Laussane, Switzerland; 2001.

[24] Federal Emergency Management Agency (FEMA). Prestandard and commentary for the seismic rehabilitation of buildings. Report FEMA 356, Washington, DC, USA; 2000.

[25] PEER. PEER NGA Online database. Accesed February/23/2009. Available from: http://peer.berkeley.edu/nga/search.html.

[26] Masi A. Seismic vulnerability assessment of gravity load designed R/C frames. Bull Earthq Eng 2003; 1(3): 371-95.

[27] Memari AM, Motlagh AY, Scanlon A. Seismic evaluation of an existing reinforced concrete framed tube building based on inelastic dynamic analysis. Eng Struct 2000; 22(6): 621-37.

[28] Ghobarah A, Abou-Elfath H, Biddah A. Response-based damage assessment of structures. Earthq Eng Struct Dyn 1999; 28(1): 79-104.

[29] Zembaty Z, Kowalski M, Pospisil S. Dynamic identification of an RC frame in progressive states of damage. Eng Struct 2006; 28(5): 668-81.

Table 1. Degradation parameters and damping ratios used in DRAIN-3DX for calibration purposes.

Parameter		Bare frame	CFRP-strengthened
Damping	1st mode	3%	5%
	2nd mode	2%	4%
Concrete unloading factor		1.0	1.0
Bond degradation factors	Stiffness, Tension and Compression	0.5	-
	Pinch, Pinch Strength and Pinch Plateau	1.0	-
Gap unloading factor		0.5	0.5

Table 2. Structural period of the frame obtained from tests and analysis (in sec)

Condition		Period 1st mode		Period 2nd mode	
		Experiments	Analysis	Experiments	Analysis
Bare	Undamaged	0.53	0.51	0.18	0.19
	After 0.05g	0.60	0.58	0.21	0.22
	After 0.20g	0.93	0.89	0.28	0.30
	After 0.40g	1.47	1.41	0.40	0.42
CFRP-strengthened	After strengthening	0.73	0.70	0.23	0.25
	After 0.05g	0.79	0.76	0.24	0.23
	After 0.20g	0.94	0.90	0.28	0.31
	After 0.40g	1.02	0.96	0.30	0.34

Table 3. Inter-storey drift results from experiments and analysis (in %)

PGA	Floor No.	Bare frame		CFRP-strengthened	
		Experiments	Analysis	Experiments	Analysis
0.05g	2	0.2	0.2	0.1	0.1
	1	0.2	0.3	0.4	0.3
0.20g	2	1.2	1.5	0.6	0.8
	1	1.4	1.3	1.3	1.3
0.40g	2	3.9	3.9	1.3	2.2
	1	1.9	1.6	2.5	2.2

Table 4. Characteristics of the real earthquake records used in the evaluation

EQ	Earthquake name	M	Station	Dist. [a] (km)	PGA (g)	Duration (s)
1	1989 Loma Prieta	6.9	Capitola	14.5	0.46	40.0
2	1989 Loma Prieta	6.9	Saratoga, Aloha Ave	12.4	0.51	40.0
3	1994 Northdridge	6.7	Canoga Pk	15.8	0.42	25.0
4	1994 Northdridge	6.7	N. Saticoy Street	13.3	0.42	30.0
5	1994 Northdridge	6.7	LA Fletcher Dr	29.5	0.24	40.0
6	1987 Superstition Hill	6.7	El Centro Imp. Co.	13.9	0.35	40.0

[a] Closest distance to fault rupture

Table 5. Performance levels of the frame according to FEMA 356, six real earthquakes

EQ	Bare condition	Damaged condition	CFRP-strengthened condition
1	CP	CP	LS
2	LS	CP	LS
3	CP	Collapse[a]	LS
4	LS	CP	LS
5	LS	CP	LS
6	CP	Collapse[a]	LS

[a] Theoretical collapse of the frame